Ecdysteroid regulation of ovarian growth and oocyte maturation in the red flour beetle, *Tribolium castaneum*

R. Parthasarathy, **Zhentao Sheng**, **Zhiyang Sun**, and **Subba R. Palli**[*]
Department of Entomology, College of Agriculture, University of Kentucky, Lexington, KY 40546

Abstract

Previous studies from our laboratory showed the involvement of juvenile hormone (JH) and ecdysteroid signaling in the regulation of female reproduction in the red flour beetle, *Tribolium castaneum*. JH regulates vitellogenin (Vg) synthesis in the fat body but the role of ecdysteroid signaling is not known. Here, we report on ecdysteroid regulation of ovarian growth and oocyte maturation. Microarray analysis of RNA isolated from ovaries showed the up-regulation of several genes coding for proteins involved in ecdysteroid signaling on the 4th day after female adult eclosion. The functional analyses of genes coding for proteins involved in ecdysteroid and JH signaling pathways by RNA interference (RNAi) revealed that ecdysteroids but not JH regulate ovarian growth and primary oocyte maturation. Ultrastructural studies showed the temporal sequences of key events in oogenesis including the development of primary oocytes, the differentiation and development of follicle epithelial cells, and the formation of intercellular spaces to facilitate uptake of Vg protein. RNAi studies showed that ecdysone receptor (EcR) and ultraspiracle (USP) are required for the ovarian growth, primary oocyte maturation and the growth and migration of the follicle cells. These studies suggest important roles for ecdysteroids in the regulation of oocyte maturation in the beetle ovaries.

Keywords

RNAi; vitellogenesis; 20E; JH; ovary; follicle cell; *Tribolium*

1. Introduction

The successful reproduction in insects encompasses the synthesis of yolk protein, vitellogenin (Vg), and its deposition into the ovary. The fat body is the major site for the synthesis of Vg proteins and the oocyte serves as a site for their uptake and assembly. The development of the ovary is generally coordinated with the other events during the post-embryonic development (Telfer, 1965). The terminal differentiation of oocyte marks the final event in oocyte maturation. The follicle cells, which form an epithelium continuously surrounding the oocyte, appear to be the most active component of the ovary during pre- and post-vitellogenic stages.

[*]Corresponding Author, Phone: 859 257 4962, Fax: 859 323 1120, RPALLI@UKY.EDU.

In most of the holometabolous insects except for a few Lepidopteran insects (Ramaswamy et al. 1997), the ovarian maturation occurs after adult eclosion. The growth of the terminal follicle, stimulation of follicular epithelium differentiation and development resulting in competence of oocyte for protein internalization constitute the most important steps in ovarian maturation. The juvenile hormone (JH) appears to control these events in *Drosophila melanogaster* (Tedesco et al. 1981) and *Aedes aegypti* (Raikhel and Lea, 1985; 1986), while 20-hydroxyecdysone (20E) regulates these events in the pharate adults (late pupal stage) of the silk moth, *Bombyx mori* (Swevers and Iatrou, 2003). Among the dipterans, the requirement of JH for ovarian maturation has been observed in *D. melanogaster*, *Musca domestica*, and several species of *Aedes* (Kelly et al. 1987). In the case of Lepidoptera, the endocrine requirements for ovarian maturation differ depending on the timing of the reproductive maturation (Belles, 1998). In *B. mori*, allatectomy (removal of corpora allata) of pupae does not prevent egg maturation (Izumi et al. 1994). However, decapitation of females after emergence resulted in the failure of production of mature oocytes in *Spodoptera frugiperda* (Sorge et al. 2000). A positive correlation between JH synthesis and ovarian development has been reported in several species of Coleoptera (Kramer, 1978; Guan and Chen, 1986; Taub-Montemayor, et al. 1997), except in the mealworm beetle, *Tenebrio molitor* (Weaver et al. 1978). Although germ-cell cluster formation in the ovary has been studied in the larval and pupal stages of the red flour beetle, *Tribolium castaneum* (Trauner and Buning, 2007), the endocrine and molecular mechanisms underlying the beetle oocyte maturation in the adult stage remain unknown.

Previous studies on the genes coding for proteins involved in JH and 20E biosynthesis and action showed that both pathways play important roles in the regulation of vitellogenesis in *T. castaneum* (Parthasarathy et al, 2010). These studies showed that JH but not 20E induced Vg synthesis in the fat body and it is not clear how 20E regulates vitellogenesis. We hypothesized that 20E might directly regulate oocyte maturation and the signals released by maturing oocytes may influence vitellogenesis. In the current study, we explored the role of genes coding for proteins involved in JH and 20E biosynthesis and action on the ovarian growth and primary oocyte maturation during the pre-vitellogenic stage of the female beetle. Especially, RNAi-aided knock-down in the expression of genes coding for proteins involved in the ecdysteroid signaling caused critical defects in the maturation of the primary oocytes and thereby egg production. Unlike the regulation of oogenesis of *Ae. aegypti* and a few lepidopteran insects belonging to Noctuidae family, where JH signaling is involved in oocyte maturation and 20E promotes Vg synthesis, we observed a reversed role of these two hormones in *T. castaneum*. These studies showed the tissue specific physiological roles of 20E, and propose a direct role for 20E in the regulation of oocyte maturation and an indirect role in the regulation of Vg synthesis in *T. castaneum*.

2. Materials and Methods

2.1. Rearing and staging

Strain GA-1 of *T. castaneum* was reared on organic wheat flour containing 10% yeast at 30°C under standard conditions as described previously (Parthasarathy et al. 2008). The pupae were separated by sex based on the structural differences of genital papillae according to *Tribolium* rearing protocol (http://bru.gmprc.ksu.edu/proj/tribolium/wrangle.asp). Adult beetles were staged soon after emergence; the adults with untanned cuticle (teneral adults) were designated as 0 h and staged thereafter.

2.2. Microarray analysis

Total RNA isolated from the whole body and ovaries dissected from staged insects were used to perform microarray analyses as described in Parthasarathy et al., 2009.

2.3. Double-stranded RNA (dsRNA) synthesis and injection

dsRNAs were synthesized using the Ambion MEGAscript transcription kit (Ambion, Austin, TX). Cognate primers designed based on the sequences available in the Beetlebase [Table 1, (Parthasarathy et al., 2010)] with T7 polymerase promoter sequence added at their 5' ends were used in PCR reactions to amplify 300–500 bp fragments of each gene. DsRNA were prepared and injected into pupae or newly ecdysed adults as described in Parthasarathy et al., 2010. The dsRNA of *Escherichia coli* maltase E (*malE*) gene was used as a control.

2.4. cDNA synthesis and Quantitative real-time reverse-transcriptase PCR (qRT-PCR)

Total RNA was extracted from the whole body or ovaries dissected from the staged adults using TRI reagent (Molecular Research Center Inc., Cincinnati, OH). cDNA was synthesized and the mRNA levels of select genes were quantified as described in Parthasarathy et al., 2010.

2.5. Mating assays

dsRNA of candidate genes were injected into the female insects at appropriate stages as described above. Four days post adult emergence (PAE), the injected virgin female beetles were mated with uninjected virgin male beetles on a single pair basis in a 24-well plate containing a layer of diet. The mating was performed under standard conditions as mentioned above. On seventh day after mating was initiated, the beetles were removed and the number of eggs laid by each pair was determined. Female beetles injected with *malE* dsRNA served as controls.

2.6. Tissue preparation, staining, and documentation

The ovaries of staged RNAi insects were dissected in 1X PBS (Phosphate-buffered saline) and fixed with 4% paraformaldehyde. The tissues were washed once with 1X PBS, then permeated with PBST (1X PBS plus 0.2% Tween-20) for 10 minutes. The tissues were stained with the nuclear stain DAPI (Sigma) for 5 min. at the dilution of 1:1000 of 1 mg/ml stock.

Ten ovaries were observed for each treatment. For fluorescent images, an Olympus FV1000 laser scanning confocal microscope was used. DAPI was excited using 405 nm laser line. The primary objective used was an Olympus water immersion PLAPO40XWLSM-NA1.0. Image acquisition was conducted at a resolution of 512×512 pixels and a scan-rate of 10 ms/pixel. Control of the microscope, as well as image acquisition and exportation as TIFF files, was conducted using Olympus Fluoview software version 1.5. Exposure settings that minimized oversaturated pixels in the final images were used. Figures of all micrographs were assembled using Photoshop 7.0.

2.7. Light and Electron microscopy

For the preparation of semi- and ultra-thin sections, ovaries were dissected in fixative (3.5% glutaraldehyde in 0.1 M sodium cacodylate buffer, pH 7.4) and fixed for 1 h at 4°C. After three rinses with 0.1 M sodium cacodylate buffer, the tissues were post fixed in 1% osmium tetroxide in buffer for 1.5 h at 4°C. Following graded dehydration in an ethanol series and two changes of propylene oxide, tissues were embedded in Eponate-12 resin (Electron Microscopy Sciences, Fort Washington, PA). Sections were cut on a Reichert-Jung Ultracut E. Semi-thin sections were stained using a 0.2% Methylene Blue, mounted in Cytoseal™ 60 mounting medium (Richard-Allan Scientific, Kalamazoo, MI) and analyzed with a Zeiss Axiophot microscope. Ultra-thin sections were contrasted with lead citrate and uranyl acetate solutions. Ultrastructural analysis was performed with a Philips Tecnai Biotwin 12 transmission electron microscope.

2.8. Statistical analysis

JMP® Start Statistics (SAS institute Inc.) version 5.1 was used for statistical analysis. The mean values of treatments versus mean values of control were compared using One way ANOVA analysis. . For comparison of the multiple means, Tukey-Kramer Honestly Significant Difference (HSD) adjustment's mean separation test was included.

3. Results

3.1. Microarray analysis

To identify highly expressed genes that may be involved in hormonal signaling and vitellogenesis in the ovary, total RNA samples isolated from the whole body or ovaries dissected from the female beetles on day 4 post adult emergence (PAE) were labeled and hybridized to *T. castaneum* custom microarrays. Three biological replicates were included for each time-point. Out of the 15,208 probe sets screened, hybridization to 12,230 probe sets was detected in at least one of the samples analyzed. The spot intensity data for these probe sets were statistically analyzed using GeneSpring software. The fold differences in expression (calculated by dividing the normalized mean values of signal intensities of the ovary samples with those of whole body samples) and the significance of difference (p-value from t-test) for 12,230 probe sets were determined. Benjamini-Hochberg false discovery rate multiple testing corrections analysis showed the expression of 962 genes at three-fold higher with a p value of <0.05 in the ovary when compared to their expression in the whole body. Among these 962 genes filtered by the Benjamini-Hochberg test, the expression levels of several genes coding for proteins known to be involved in vitellogenesis, 20E, and JH signaling pathways compared between the ovary and whole body are shown in Table 1. Some of the genes known to be involved in these signaling pathways with a fold difference of greater than two and a p value less than 0.05 were also included. Interestingly, the expression of genes coding for vitellogenin receptors (VgR1 and VgR2) were detected at 6.5- and 4-fold higher respectively in the ovary than in the whole body. The expression of genes coding for enzymes (Phantom, Shade, Shadow, Spookier and disembodied) known to be involved in ecdysteroid biosynthesis were also detected at two to four-fold higher in the ovary than in the whole body samples. Similarly, the expression of genes coding for proteins (EcR, E78, and HR78) known to be involved in 20E action were present at two-fold higher in the ovary than in the whole body samples. The genes coding for enzymes known to be involved in JH metabolism such as JHE and JHEH were 2.7 to 8-fold higher respectively in the ovary than in the whole body. The genes coding for proteins involved in JH biosynthesis (JHAMT, JH acid methyl transferase), JH action (Met, Methoprene tolerant; Kr-h1, Kruppel), and ecdysteroid action (EcR and USP) did not show more than 2-fold higher expression in the ovary than in the whole body and hence are not shown in Table 1.

Out of the 962 genes filtered by Benjamini-Hochberg false discovery rate multiple testing, 584 genes showed expression levels of 3-fold higher in the ovary when compared to their expression in the whole body with a p-value of <0.001. These genes were further analyzed using the Blast2go (http://www.blast2go.org) program based on their annotations on molecular functions. These genes were grouped into 14 molecular functional categories (Fig. 1). The most important categories recognized were DNA and protein binding, signal transduction, transcriptional activity, and transmembrane activity. Interestingly, a majority of genes were grouped into protein binding and nucleic acid binding (22 % each) activities, followed by signal transduction and transcriptional activity (5% each), and transmembrane transporter activity (1.10 %). These functional classification of genes highly expressed in the ovary suggests high DNA binding and protein binding activities involved in oogenesis on day 4 PAE.

We also compared putative ovarian specific genes identified in our microarray analysis with the genes reported to be involved in *D. melanogaster* egg development (Baker and Russell, 2009). Fourteen genes that are expressed in the *T. castaneum* ovary (at more than 1.5-fold higher in the ovary when compared to their expression in the whole body with a p-value of less than 0.01) and identified as those involved in *D. melanogaster* egg development are shown in Table 2.

3.2. Expression of select genes in the ovary

The expression levels of select genes coding for proteins involved in JH and 20E action were determined in the ovary during 0–5 days PAE by qRT-PCR (Fig. 2). JHAMT and Phantom are hormone biosynthetic enzymes expressed mainly in the endocrine glands, their expression levels were too low in the ovary (data not shown). Met mRNA levels were high on day 0 PAE and the levels declined steadily during next four days. In contrast, Kr-h1 mRNA levels increased steadily from 0–5 days PAE in the ovary. Shade mRNA levels showed a peak on day 1 PAE in the ovary and declined significantly during 2–5 days PAE. EcR and USP levels did not vary significantly during 0–5 days PAE. The expression patterns of the Vg receptors, VgR1 and VgR2 in the ovary were similar during 0–5 days PAE (Fig. 2). The expression of both receptors steadily increased after day 1 PAE and reached the peak levels by day 4 PAE and the expression levels remained high during 4–5 days PAE.

3.3. Effect of knock-down in the expression of genes coding for proteins involved in JH and 20E biosynthesis/action on egg production

A few genes involved in JH and 20E biosynthesis and action were selected for RNAi studies to determine their roles in female reproduction especially oogenesis. Injection of JHAMT, Met, Kr-h1, Phantom, Shade, EcR and USP dsRNA into late pupae or newly eclosed adults resulted in 60–100% reduction in their mRNA levels in four-day-old female beetles (Fig. 3A). The knock-down in the expression of genes coding for JHAMT, Met, and Kr-h1 reduced egg production by 72.4%, 91.0%, and 46.3% respectively when compared to the eggs produced by control beetles (Fig. 3B). Phantom RNAi did not affect egg production that much as only 14.3% less eggs were produced by these beetles when compared to the control beetles. Knock-down in the expression of gene coding for Shade caused a drastic reduction in the egg production by 84.3% when compared to the control beetles. Though the knock-down efficiency of both Phantom and Shade were greater than 90%, they showed different effects on egg production. Interestingly, knock-down in the expression of genes coding for EcR and USP rendered beetles sterile and no eggs were produced by these beetles. These data show that both JH and 20E are required for eggs production. To determine the functions of JH and 20E in oogenesis, detailed studies as described below are conducted on oocyte maturation.

3.4. Ovarian growth and oocyte maturation

T. castaneum ovary belongs to the category of telotrophic meroistic similar to that of yellow mealworm, *Tenebrio molitor*, the nurse cells are located at the distal end and the developing oocytes at the proximal end of the each ovariole. The ovary shows asynchronous development, however, the primary oocytes mature simultaneously in majority of the ovarioles of an ovary. The development and maturation of primary oocyte of such ovarioles were studied. Primary oocytes were staged following the nomenclature used in *T. molitor* (Ullmann, 1973). Briefly, Stage 1: primary oocyte dormant, prefollicular, located in the posterior portion of the germarium; Stage 2: primary oocyte situated in the neck region of the ovariole, several oocytes found side by side surrounded by prefollicular tissue; Stage 3: oocyte enlarges, follicles arrange one behind the other; Stage 4: spherical oocyte, nucleus transforms into germinal vesicle; Stage 5: Germinal vesicle central, follicle cells organize

into columnar epithelium; Stage 6: Yolk deposition begins, rapid increase of oocyte size, spaces appear between follicular epithelium; Stage 7: Maximum patency and yolk deposition; Stage 8: yolk deposition ceases; follicle deforms, chorion secretion begins.

The ovarioles were dissected and the morphological changes were observed from 0 h – 120 h PAE (day 0 – day 5 PAE). Tremendous changes in the ovariole morphology occurred during 60 h – 102 h PAE (day 2 – day 4 PAE), and hence the ovarioles of these stages were stained with nuclear stain, DAPI and shown in Figure 4A (a–f). At 60 h PAE, the oocytes were dormant and arranged side by side in the neck region of the ovariole. The follicular epithelial cells were undistinguishable (Stage 1–2, Fig. 4A, a). The primary oocyte was distinguished at 72 h PAE which enlarges slightly and the follicular epithelial cells increase in number covering the primary oocyte (Stage 3, Fig. 4A, b). At 84 h PAE, the primary oocyte further enlarges in size and the follicular epithelial cells were seen arranged around the oocyte (Stage 4, Fig. 4A, c). At 90 h – 96 h PAE, the primary oocyte becomes spherical and then elongates and covered by a monolayer of follicular epithelial cells (Stage 5, Fig. 4A, d–e). At this stage the germinal vesicle was seen at the center of the primary oocyte (data not shown). At 102 h PAE, the primary oocyte enters the vitellogenic phase with an increase in spacing between the follicular epithelial cells and uptake of Vg protein occurs after this stage (Stage 6, Fig. 4A, f).

To show the different regions of the ovariole, the ultra thin section of the ovariole dissected from five day-old beetle with oocytes at different developmental stages were stained with methylene blue and photographed under a microscope (Fig. 4A, panels A&B). By day 5 PAE, all the regions of the ovariole were distinct. The primary oocyte is located in the vitellarium region, the developing secondary and tertiary oocytes are located in the germarium region and the nurse cells are located in the tropharium region of the ovariole. The primary oocyte matured well; a well defined columnar follicle epithelial layer was formed and yolk uptake was completed (Fig. 4B, panel B). The secondary oocyte in this ovariole is at the intermediate stage of development; a well defined columnar follicle epithelial layer was formed and but yolk uptake was not completed (Fig. 4B, panel A). Above the secondary oocyte, the tertiary oocytes were present in the neck region of the ovariole (Fig. 4B, panel A). The top region of the ovariole was occupied by nurse cells (Fig. 4B, panel A).

The changes in the follicular epithelium of the developing primary oocytes were documented by ultra structural studies (Fig. 4B, C–E). The follicle cells become columnar and arrange to form a monolayer covering the Stage 5 primary oocyte. A well defined follicular membrane is observed embracing the follicle cells (Fig. 4B, panel C). At Stage 6, the shrinkage of follicle cells surrounding the primary oocyte is observed, this leads to the formation of intercellular spaces between the follicle cells (Fig. 4B, panel D). The follicle cells become flat with the reduction of intercellular spaces at Stage 7 of the primary oocyte and the yolk granules were observed in the ooplasm (Fig. 4B, panel E).

3.5. Effect of RNAi on ovarian growth and maturation

Having observed the growth and maturation of primary oocyte during 2–5 days PAE, the effect of RNAi of select genes on these processes were studied. dsRNA of select genes were injected and the ovaries were observed on day 4 PAE after staining with DAPI (Fig. 5A, a–h). Ovaries from beetles injected with *malE* dsRNA served as controls. In the control beetles, the primary oocytes were well developed in most of the ovarioles and were at Stage 5. The primary oocyte contained well developed follicular epithelial cells and germinal vesicle was located at the center (Fig. 5A, a). Interestingly, the knock-down in the expression of genes coding for JHAMT, Met, and Kr-h1 involved in JH biosynthesis and action, did not block the ovariole development and the maturation of the primary oocyte

(Fig. 5A, b–d). The maturation of the primary oocytes in the ovaries dissected from JHAMT and Met RNAi beetles was on par with the primary oocytes dissected from the control beetles. The primary oocytes in the ovaries dissected from Kr-h1 RNAi beetles were at Stage 4 (Fig. 5A, b–d). Among the ecdysteroid pathway genes studied, Phantom RNAi did not block primary oocyte maturation and the stage of the oocytes was similar to that observed in the control beetle ovaries (Fig. 5A, e). However, Shade, EcR, and USP RNAi severely affected the maturation of the primary oocytes and the primary oocytes maturation was blocked at Stage 2 (Fig. 5A, f–h).

To further investigate the role of 20E signaling in oocyte maturation, the EcR RNAi and *malE* RNAi (control) beetles were fed continuously for eight days and the ovariole growth at the end of the day 4 and day 8 PAE was observed. For comparison, ovarioles of JHAMT RNAi beetles were included (Fig. 5B, a–d). On day 4 PAE, in the control beetle ovariole, the primary oocyte was observed at Stage 5 (Fig. 5B, a), whereas, in the ovarioles dissected from EcR RNAi beetle the primary oocyte growth was blocked at stage 2 and the oocytes remained in the germarium region (Fig. 5B, b). On the day 8 PAE, the ovarioles dissected from EcR RNAi beetles showed a number of small oocytes arranged end to end in the germarium region (Fig. 5B, c). The development of ovarioles dissected from JHAMT RNAi beetles on day 4 PAE were on par with those in the control beetles (Fig. 5B, d).

3.6. Role of 20E signaling on ovarian growth and oocyte maturation

Detailed analysis at the cellular level was conducted to understand the role of 20E signaling on the ovarian growth and oocyte maturation using electron microscopy. The germarium regions of the ovarioles dissected from *malE* RNAi (control) and EcR RNAi beetles on day 4 PAE were investigated further by cutting ultrathin sections and observing them under an electron microscope (Fig. 6, A–D). The growth of the primary oocytes in the germarium region of EcR RNAi beetle ovariole was comparable to the growth of the secondary oocytes in the germarium region of the *malE* RNAi beetle ovariole. In the control beetle ovariole, a well developed stage 5 primary oocyte surrounded by follicular epithelial cells was observed below the vitellarium region (data not shown). A developing secondary oocyte was seen surrounded by follicular epithelial cells in the germarium region (Fig. 6, panel A). This secondary oocyte was flanked by the migrated follicular epithelial cells (Fig. 6, panel B). The ovariole of the EcR RNAi beetles consisted of mainly tropharium and a small germarium region (Fig. 7, panel C). In the germarium region, smaller primary oocytes blocked at stage 2 of development were observed (Fig. 6, panel C). A few follicular epithelial cells were present near these oocytes but these cells were not organized to surround the oocyte (Fig. 6, panel D). These data showed both the oocyte and follicular epithelial cells are present in control as well as EcR RNAi insects but the growth of the oocyte and migration of follicular epithelial cells are blocked in EcR RNAi insects.

4. Discussion

Our previous study showed that JH plays a predominant role in the regulation of Vg synthesis in the fat body. However, knock-down of 20E signaling pathway genes also blocked the Vg synthesis (Parthasarathy et al. 2010). It is not clear how 20E influences vg synthesis. The most significant contribution of the current study is the uncovering of 20E regulation of ovarian growth, oocyte maturation and follicle cell differentiation and development in *T. castaneum*, which indirectly affects Vg synthesis.

Our microarray data supported the above conclusions with the high expression of genes involved in 20E biosynthesis and action in the ovaries. By analyzing the homologues of genes known to be involved in the egg production of *D. melanogaster* by microarray analysis (Baker and Russell, 2009), we identified putative ovarian specific genes that were

highly expressed in *T. castaneum* ovaries. Based on the molecular function annotations, several genes involved in nucleic acid binding, protein binding, and transcription factor activity were highly expressed in the ovaries at day 4 PAE. Similar observations were made in the microarray analysis of *D. melanogaster* egg development study (Baker and Russell, 2009) and these groups were categorized in to the biological processes of oogenesis, cell cycle, DNA and protein catabolism.

The endocrine regulation of the ovarian growth, oocyte maturation and vitellogenesis in insects has been recognized for a long time (Engelmann, 1968, Raikhel and Dhadialla, 1992). JH regulates previtellogenic ovarian development in most insects (Tedesco et al. 1981; Hagedorn, 1994; Klowden, 1997). Topical application of a JH analog stimulated the growth of previtellogenic ovaries in decapitated or CA-ablated teneral female mosquito (Gwadz and Spielman, 1973; Hagedron et al. 1977; Hernandez-Martinez et al. 2007). JH levels increase during the first day after adult emergence and remain high correlating with the growth of the primary follicles in *Ae. aegpti* (Feinsod and Spielman, 1980; Klowden, 1997). The implantation and ablation experiments in *Ae. aegypti* clearly showed that JH is necessary for ovarian maturation (Borovsky et al., 1985). Similarly ablation experiments in *M. domestica* showed that CA is required for complete ovarian maturation (Lea, 1975). Also, the defective CA mutants of *D. melanogaster*, *apterous*, contained non-vitellogenic ovaries indicating the block in the ovarian development (Wilson, 1982; Kelly et al. 1987). JH is necessary for developmental events leading to mature eggs in most of the lepidopterans except *B. mori* (Sorge et al. 2000). In the present study, knock-down in the expression of genes coding for enzyme involved in JH biosynthesis, JHAMT or a transcription factor involved in JH action, Met did not block the follicle epithelium formation and maturation of the primary oocyte, suggesting that JH signaling is not likely involved in the ovarian growth and oocyte maturation in *T. castaneum*. Weaver et al. (1978) found no correlation between JH production and oocyte development in another tenebrionid beetle, *Tenebrio molitor*. These data clearly indicates that JH does not play a major role in oocyte maturation in the tenebrionid beetles as opposed to the effect observed in most of the dipteran, lepidopteran, and other coleopteran insects. We speculated that 20E signaling might be involved in ovarian maturation processes.

The ecdysteroid titer declined rapidly during the previtellogenic stage corroborating with the diminishing mRNA levels of Phantom (Parthasarathy et al., 2010), an enzyme involved in ecdysteroid biosynthesis (Warren, et al. 2004). Phantom RNAi did not block oocyte maturation and egg/progeny production indicating that ecdysteroid production is not required to initiate these events. Since Phantom dsRNA was injected into the day 0 PAE adults and ecdysteroid levels were very low during 3–5 days PAE, we did not estimate ecdysteroid levels in the Phantom RNAi insects. Instead, ecdysterioid synthesis and release by the ovaries dissected from Phantom or *malE* dsRNA injected beetles was determined. Ovaries dissected from Phantom RNAi insects and cultured *in vitro* produced 70–80% less ecdysteroids than the ovaries dissected from *malE* RNAi insects (control) (data not shown), suggesting that Phantom RNAi in adults blocks new ecdysteroid synthesis. Knock-down in the expression of genes coding for Shade (an enzyme involved in conversion of ecdysone to functional 20E, Petryck et al. 2003), EcR and USP (heterodimer of nuclear receptors to which 20E binds) severely impaired the ovarian growth and primary oocyte maturation, as the ovaries did not pass through Stage 2 of development by day 4 PAE. The primary oocytes in control insects completed maturation by this time. The ovarioles dissected from EcR RNAi beetles on day 8 PAE showed several smaller oocytes without well defined follicular epithelial layers around them. These data showed that the EcR RNAi does not affect oocyte/ follicle cell production but it blocks ovary growth and oocyte maturation. To elucidate the exact role of ecdysteroid signaling in the oocyte maturation, the ultrastructural analyses were performed. These studies revealed the differentiation of follicle cells and migration of these

cells flanking the developing oocytes in the germarium region of the control beetle ovariole. The oocyte flanked by follicle cells leave the germarium to mature as primary oocytes in the vitellarium. In EcR RNAi ovariole, the presence of follicular cells around the developing primary oocyte in the germarium region were observed on day 4 PAE; however, the follicle cells failed to migrate and arrange as a monolayer surrounding the primary oocyte leading to formation of several smaller naked oocytes without follicle cells around them.

The involvement of EcR signaling in the follicular epithelial cell differentiation has been reported in other insect species (Belles et al. 1993; Carney and Bender, 2000; Cruz et al. 2006, Sun et al. 2008). Hackney et al. (2007) showed that EcR modulates follicle cell differentiation including cell migrations and chorion gene expression and amplification during late oogenesis in *D. melanogaster*. Recently, using reverse genetic analysis of EcR-B1 isoform in *D. melanogaster*, it was shown that EcR B1 isoform is required for proper follicle cell polarity both during the early stages of oogenesis, when follicle cells undergo mitotic cycle; at mid-oogenesis when these cells stop dividing and undergo several endocycles. Also, this study reported that EcR-B1 isoform is required for follicle cell survival and that disruption of its function caused apoptotic cell death induced by caspases (Romani et al. 2009). Similar to the phenotypes observed in EcR RNAi and *EcR* mutants of *D. melanogaster*, the depletion of EcR by RNAi in the female beetles might have induced apoptosis of the follicular epithelial cells in *T. castaneum*. In accordance with the data from *D. melanogaster*, our data on RNAi of genes coding for proteins involved in 20E signaling point to the involvement of the existing ecdysteroids that are converted to 20E by Shade then the 20E acts through EcR/USP in the ovary to promote the follicular epithelial differentiation and the maturation of the primary oocytes. As observed in *T. molitor* (Ullmann, 1973) and other insects (Telfer, 1965), the follicle cells contribute to the ooplasm and result in an increase of primary oocyte size in *T. castaneum*. Absence of follicle cells differentiation in EcR RNAi beetles might have resulted in the failure to increase in the size of the oocytes, leading to the failure in the maturation of primary oocytes.

In insects such as *Blatella germanica*, where vitellogenesis is strictly dependent on JH but not ecdysteroid, knocking down the expression of BgEcRA levels during the adult stage did not alter the hemolymph or the ovarian levels of vitellogenenin/vitellin (Cruz et al. 2006). Surprisingly, in the case of *T. castaneum*, Shade, EcR, and USP RNAi affected Vg transcription (Parthasarathy et al., 2010) and egg production. Elliot et al. (2006) showed that ovaries at a specific stage of development release an ovarian factor that stimulates JH synthesis in the corpora allata of *Diploptera punctata*. In our study, the timing of the follicle cell differentiation and maturation of primary oocyte coincides with the peak activity of JH followed by the initiation of Vg gene expression. We propose that failure to initiate Vg transcription in the fat body of EcR, USP, and Shade RNAi insects is not a direct action of 20E signaling in the fat body; rather it is an indirect effect caused by the arrest of ovarian growth and maturation mediated by 20E signaling in the ovaries, which in turn, blocks Vg synthesis and egg production.

Our data on egg production clearly confirmed the functional roles of the genes in the oogenesis irrespective of the knock-down efficiency of particular gene. Interestingly, knock-down in the expression of genes coding for proteins involved in JH biosynthesis and action blocked egg production. Since, knock-down in the expression of genes coding for proteins involved in JH biosynthesis or action did not block oocyte maturation, it is likely that the suppressive effect of JH on egg production is due to the reduced level of Vg synthesis observed in JHAMT, Met, and Kr-h1 RNAi insects (Parthasarathy et al., 2010).

Taken together these studies showed that 20E and its receptors are required for ovary growth, oocyte maturation and follicle cell differentiation and development. The matured

oocytes signal for the initiation of Vg gene expression in the fat body. The Vg gene expression in the fat body is regulated by JH (Parthasarathy et al., 2010). The nature of signals released by ovary to initiate Vg gene expression in the fat body is likely peptides but they remain unidentified and are currently under investigation. The present study in conjunction with the study on JH regulation of Vg synthesis (Parthasarathy et al., 2010) provide solid foundation for future studies to understand the molecular mechanisms of regulation of reproduction in beetles.

Acknowledgments

References

Baker DA, Russell S. Gene expression during *Drosophila melanogaster* egg development before and after reproductive diapuase. BMC Genomics 2009;10:242. doi:10.1 186/1471-2164-10-242. [PubMed: 19463195]

Belles, X. Endocrine effectors in insect vitellogenesis. In: Coast, GM.; Webster, SG., editors. Recent advances in arthropod endocrinology. Cambridge University Press; 1998. p. 68-90.

Belles X, Cassier P, Cerda X, Pascaul N, Andre M, Rosso Y, Piulachs MD. Induction of choriogenesis by 20-hydroxyecdysone in the german cockroach. Tissue Cell 1993;25:195–204. [PubMed: 18621230]

Borovsky D, Thomas BR, Carlson DA, Whisenton LR, Fuchs MS. Juvenile hormone and 20-hydroxyecdysone as primary and secondary stimuli of vitellogenesis in *Aedes aegypti*. Arch. Insect Biochem. Physiol 1985;2:75–90.

Carney GE, Bender M. The *Drosophila* ecdysone receptor (EcR) gene is required maternally for normal oogenesis. Genetics 2000;154:1203–1211. [PubMed: 10757764]

Cruz JD, Mane-Padros D, Belles X, Martin D. Functions of the ecdysone receptor isoform-A in the hemimetabolous insect *Blattella germanica* revealed by systemic RNAi in vivo. Dev. Biol 2006;297:158–171. [PubMed: 16890931]

Elliott KL, Woodhead AP, Stay B. A stage-specific ovarian factor with stable stimulation of juvenile hormone synthesis in corpora allata of the cockroach, *Diploptera punctata*. J. Insect Physiol 2006;52:929–935. [PubMed: 16890239]

Engelmann F. Endocrine control of insect reproduction. Annu. Rev. Entomol 1968;13:1–26.

Feinsod FM, Spielman A. Nutrient-mediated juvenile hormone secretion in mosquitoes. J. Insect Physiol 1980;26:113–117.

Guam XC, Chen EY. Corpus allatum activity in the female *Coccinella septempunctata* adults. Acta Entomol. Sinica 1986;29:10–24.

Gwadz RW, Spielman A. Corpus allatum control of ovarian development in *Aedes aegypti*. J. Insect Physiol 1973;19:1441–1448. [PubMed: 4720505]

Hackney JF, Pucci C, Naes E, Dobens L. Ras signaling modulates activity of the ecdysone receptor EcR during cell migration in the *Drosophila* ovary. Dev. Dyn 2007;236:1213–1226. [PubMed: 17436275]

Hagedorn HH. The endocrinology of the adult female mosquito. Adv. Disease Vec. Res 1994;10:109–148.

Hagedorn HH, Turner S, Hagedron EA, Pontecorvo D, Greenbaun P, Pfeiffer D, Wheelock G, Flanagan TR. Postemergence growth of the ovarian follicles of *Aedes aegypti*. J. Insect Physiol 1977;23:203–206. [PubMed: 558249]

Hernandez-Martinez S, Mayoral JG, Li Y, Noriega FG. Role of juvenile hormone and allatropin on nutrient allocation, ovarian development and survivorship in mosquitoes. J. Insect Physiol 2007;53:230–234. [PubMed: 17070832]

Izumi S, Yano K, Yamamoto Y, Takahashi SY. Yolk proteins from insect eggs: structure, biosynthesis and programmed degradation during embryogenesis. J. Insect Physiol 1994;40:735–746.

Kelly TJ, Adams TS, Schwartz MB, Birnbaum MJ, Rubenstein EC, Imberski RB. Juvenile hormone and ovarian maturation in the dipteral: A review of recent results. Insect Biochem 1987;17:1089–1093.

Klowden MJ. Endocrine aspects of mosquito reproduction. Arch. Insect Biochem. Physiol 1997;35:491–512.

Kramer SJ. Age-dependent changes in corpus activity in vitro in the adult Colorado potato beetle, *Leptinotarsa decemlineata*. J. Insect Physiol 1978;24:461–464.

Lassiter MT, Apperson CS, Crawford CL. Juvenile hormone metabolism during adult development of Culex quinquefasciatus (Diptera: Culicidae). J. Med. Entomol 1994;31:586–593. [PubMed: 7932605]

Lea AO. Evidence that the ovaries of *Musca domestica* do not maintain cyclicity by regulating the corpus allatum. J. Insect Physiol 1975;21:1747–1750. [PubMed: 1184999]

Parthasarathy R, Tan A, Bai H, Palli SR. Transcription factor broad suppresses precocious development of adult structures during larval-pupal metamorphosis in the red flour beetle, *Tribolium castaneum*. Mech. Dev 2008;125:299–313. [PubMed: 18083350]

Parthasarathy R, Tan A, Sun Z, Chen J, Rainkin M, Palli SR. Juvenile hormone regulation of male accessory gland activity in the red flour beetle, *Tribolium castaneum*. Mech. Dev 2009;126:563–579. [PubMed: 19324087]

Parthasarathy R, Sun Z, Bai H, Palli SR. Juvenile hormone regulation of vitellogenin synthesis in the red flour beetle, *Tribolium castaneum*. Insect Biochem. Mol. Biol. 2010 In Press.

Petryk A, Warren JT, Marques G, Jarcho MP, Gilbert LI, Kahler J, Parvy JP, Li Y, Dauphin-Villemant C, O'Connor MB. Shade is the *Drosophila* p450 enzyme that mediates the hydroxylation of ecdysone to the steroid insect molting hormone 20E-hydroxyecdysone. Proc. Natl. Acad. Sci. U. S. A 2003;111:13773–13778. [PubMed: 14610274]

Raikhel AS, Dhadialla TS. Accumulation of yolk proteins in insect oocytes. Annu. Rev. Entomol 1992;37:217–251. [PubMed: 1311540]

Raikhel AS, Lea AO. Hormone-mediated formation of the endocytic complex in mosquito oocytes. Gen. Comp. Endocrinol 1985;53:424–435.

Raikhel AS, Lea AO. The specific ligand, vitellogenin, directs internalized proteins into accumulative compartments of mosquito oocytes. Tissue Cell 1986;18:559–574. [PubMed: 3750316]

Ramaswamy SB, Shu S, Park YL, Zeng F. Dynamics of juvenile hormone-mediated gonadotropism in the Lepidoptera. Arch. Insect Biochem. Physiol 1997;35:539–558.

Romani P, Bernardi F, Hackney J, Dobens L, Gargiulo g, Cavaliere V. Cell survival and polarity of *Drosophila* follicle cells require the activity of ecdysone receptor B1 isoform. Genetics 2009;181:165–175. [PubMed: 19015542]

Sorge D, Nauen R, Range S, Hoffmann KH. Regulation of vitellogenesis in the fall armyworm, *Spodoptera frugiperda* (Lepidoptera: Noctuidae). J. Insect Physiol 2000;46:969–976. [PubMed: 10802110]

Sun J, Smith L, Armento A, Deng W. Regulation of the endocycle/gene amplification switch by Notch and ecdysone signaling. J. Cell Biol 2008;182:885–896. [PubMed: 18779369]

Swevers L, Iatrou K. The ecdysone regulatory cascade and ovarian development in lepidopteran insects: insights from the silkmoth paradigm. Insect Biochem. Mol. Biol 2003;33:1285–1297. [PubMed: 14599500]

Taub-Montemayor, Te; Dahm, KH.; Bhaskaran, G.; Rankin, MA. Rates of juvenile hormone biosynthesis and degradation during reproductive development and diapause in the boll weevil, *Anthonomas grandis*. Physiol. Entomol 1997;22:269–276.

Tedesco JL, Courtright JB, Kumaran AK. Ultrastructural changes induced by juvenile hormone analogue in oocyte membranes of apterous *Drosophila melanogaster*. J. Insect Physiol 1981;27:895–902.

Telfer WH. The mechanism and control of yolk formation. Annu. Rev. Entomol 1965;10:161–184.

Trauner J, Buning J. Germ-cell cluster formation in the telotrophic meroistic ovary of *Tribolium castaneum* (Coleoptera, Polyphaga, Tenebrionidae) and its implication on insect phylogeny. Dev. Genes Evol 2007;217:13–27. [PubMed: 17123126]

Ullmann SL. Oogenesis in *Tenebrio molitor*: histological and autoradiographical observations on pupal and adult ovaries. J. Embryol. Exp. Morphol 1973;30:179–217. [PubMed: 4729945]

Warren JT, Petryk A, Marques G, Parvy JP, Shinoda T, Itoyama K, Kobayashi J, Jarcho M, Li Y, O'Connor MB, Dauphin-Villemant C, Gilbert LI. Phantom encodes the 25-hydroxylase of *Drosophila melanogaster* and *Bombyx mori*: a P450 enzyme critical in ecdysone biosynthesis. Insect Biochem. Mol. Biol 2004;34:991–1010. [PubMed: 15350618]

Weaver RJ, Pratt GE, Hamnett AF. Radiochemical assays of juvenile hormone biosynthesis by cultured corpora allata in relation to oogenesis in the beetle, *Tenebrio molitor*, and the cockroach, *Periplaneta americana*. Gen. Comp. Endocrinol 1978;34:112–113.

Wilson TG. A correlation between juvenile hormone and vitellogenic oocyte degeneration in *Drosophila melamogaster*. Dev. Gene Evol 1982;191:257–263.
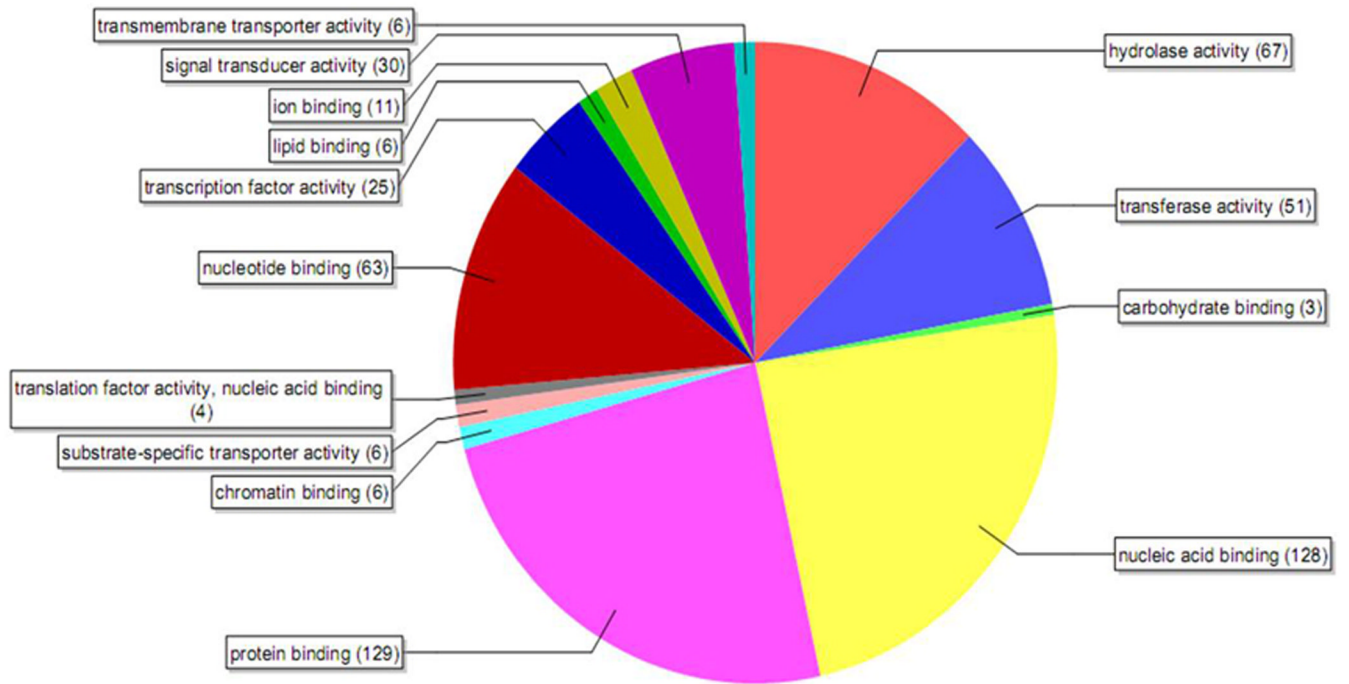
Fig. 1.
Pie-chart showing the distribution of genes based on their annotations on molecular functions using Blast2go software. Microarray analysis was done with RNA samples from day 4 PAE ovary tissues and whole body. The genes filtered by Bejamini- Hochberg analysis that were 3-fold higher in the ovary when compared to their expression in the whole body with a p-value of <0.001 were considered.
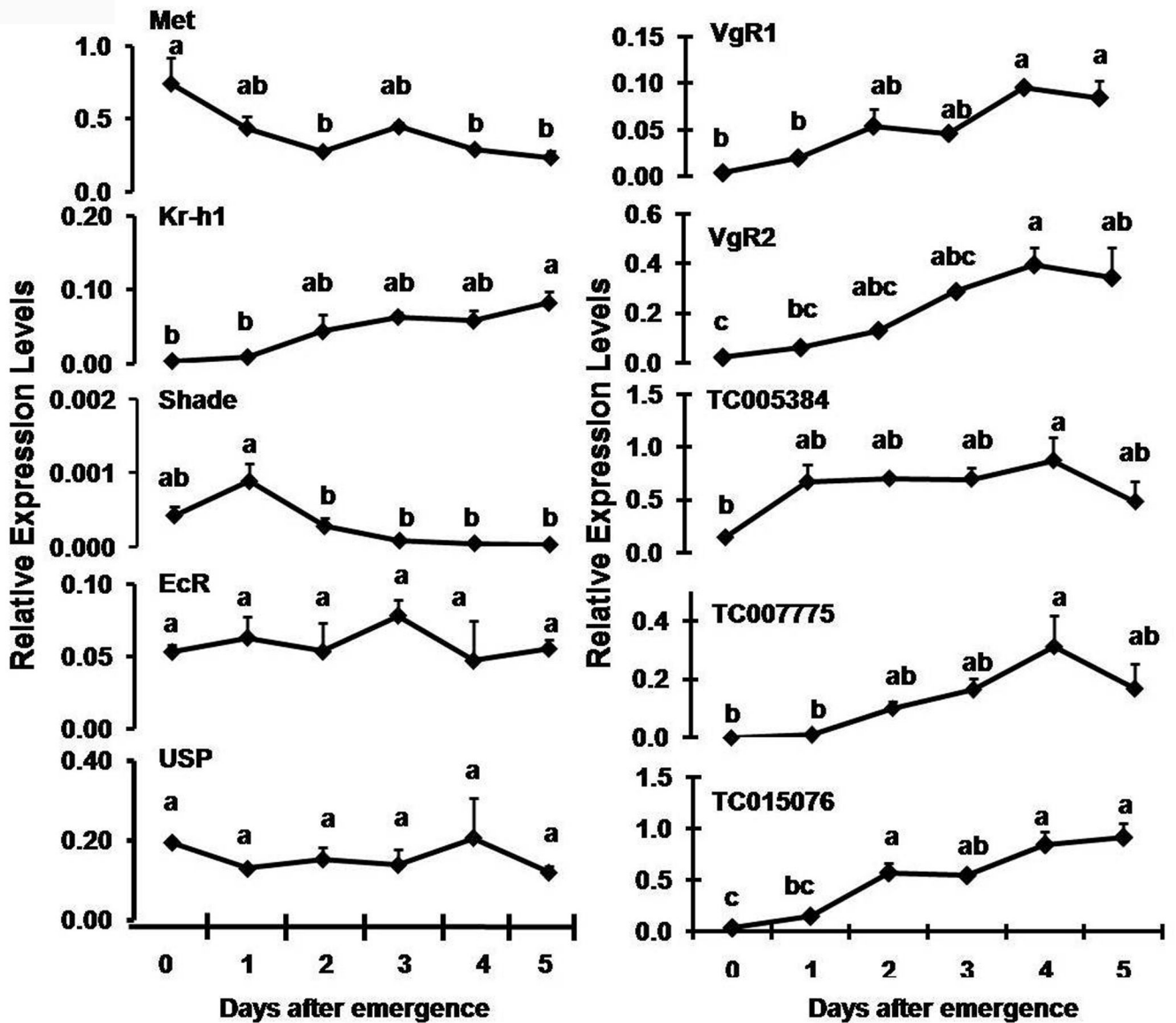
Fig. 2.
Relative expression levels of select genes in the ovaries during 0–5 days PAE were determined by qRT-PCR. RNA was extracted from the ovaries at specific time-points. Relative expression in comparison to ribosomal protein (rp49) gene expression was determined. Mean ± S.E. of three independent replicates are shown. One-way ANOVA analysis was performed using JMP software (SAS institute). The mean expression levels marked with the same alphabetical letter do not differ significantly at p<0.05.
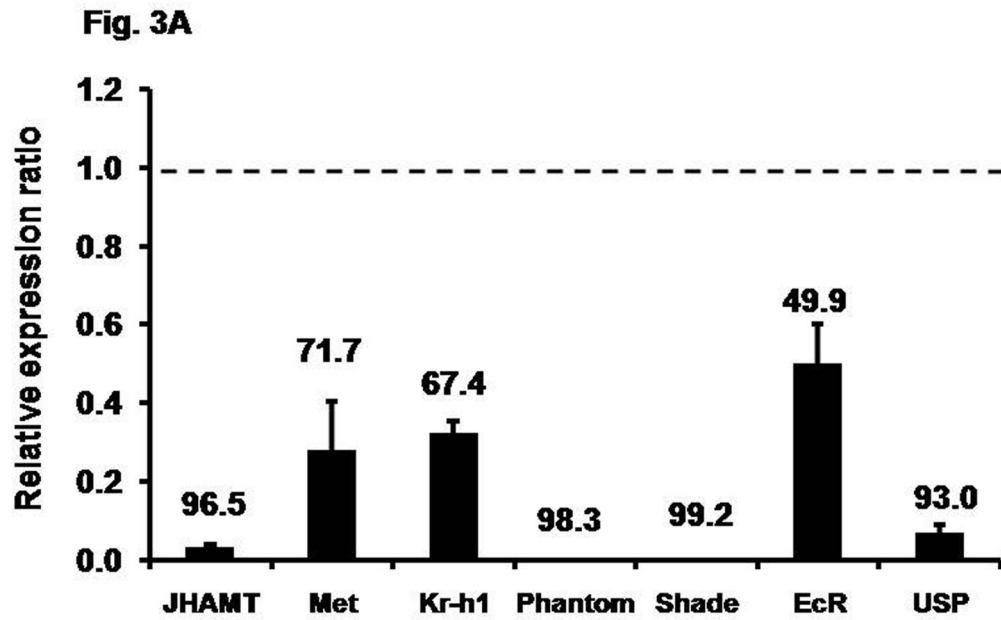
Fig. 3A

Fig. 3B
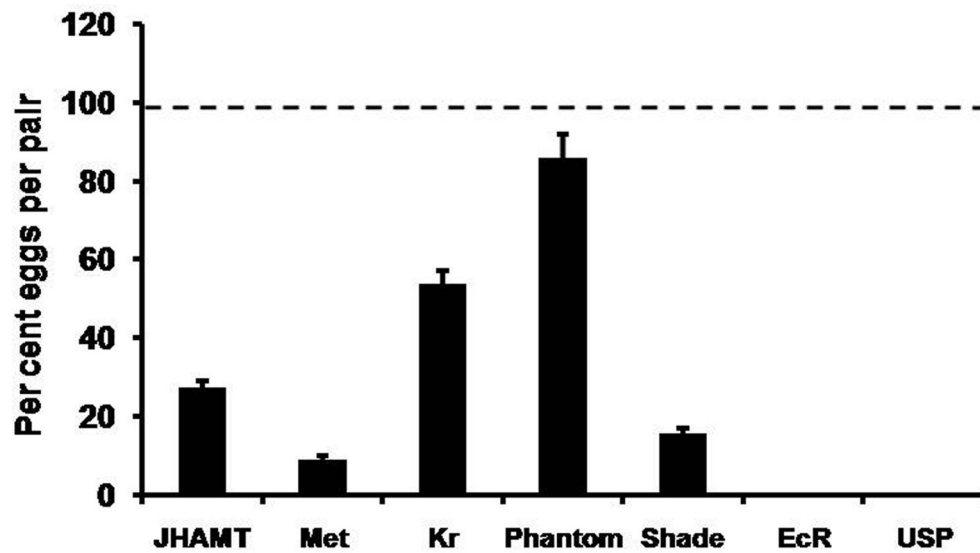
Fig. 3.
Fig. 3A. Knock-down efficiency of gene expression after injection of dsRNA. dsRNA for genes coding for proteins involved in JH biosynthesis or action (JHAMT, Met, Kr-h1), 20E biosynthesis and action (Phantom, Shade, EcR, USP) and *malE* (control) were injected into two-day-old female pupae or day 0 PAE adults (within 24 h of emergence). On day 4 PAE, RNA was extracted and the relative expression in comparison to ribosomal protein (rp49) was determined by qRT-PCR. The expression levels of these respective genes in the control insects were set to 1, the relative expression levels were determined with respect to control, and the numbers above each bar show the percent knock-down efficiency. Mean ± S.E. of three independent replicates are shown.

Fig. 3B. Effect of knock-down in the expression of genes involved in JH biosynthesis and action (JHAMT, Met , Kr-h1) and 20E biosynthesis and action (Phantom, Shade, EcR, USP) on the number of eggs produced by RNAi females mated with uninjected virgin males. dsRNAs of the above genes were injected as described in the Materials and Methods section. On the 4th day after adult eclosion, the RNAi females were mated with the virgin males on a single pair basis. The average numbers of eggs from each pair were shown. The egg produced by female beetles injected with *malE* dsRNA served as a control and set as 100 percent. The percent eggs produced with respect to control was determined for each treatment. Mean ± S.E. of three independent replicates with 10 pairs in each replicate are shown.

Fig. 4A
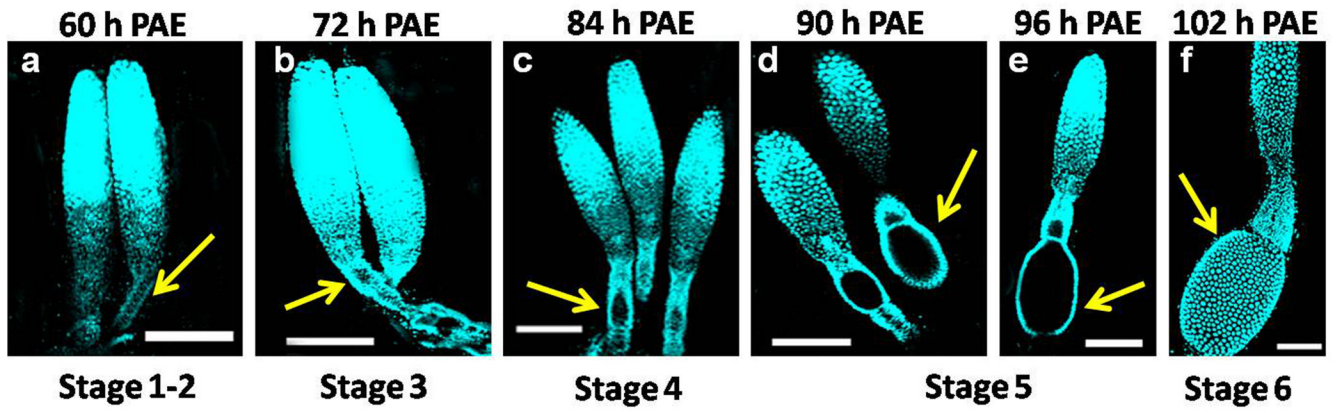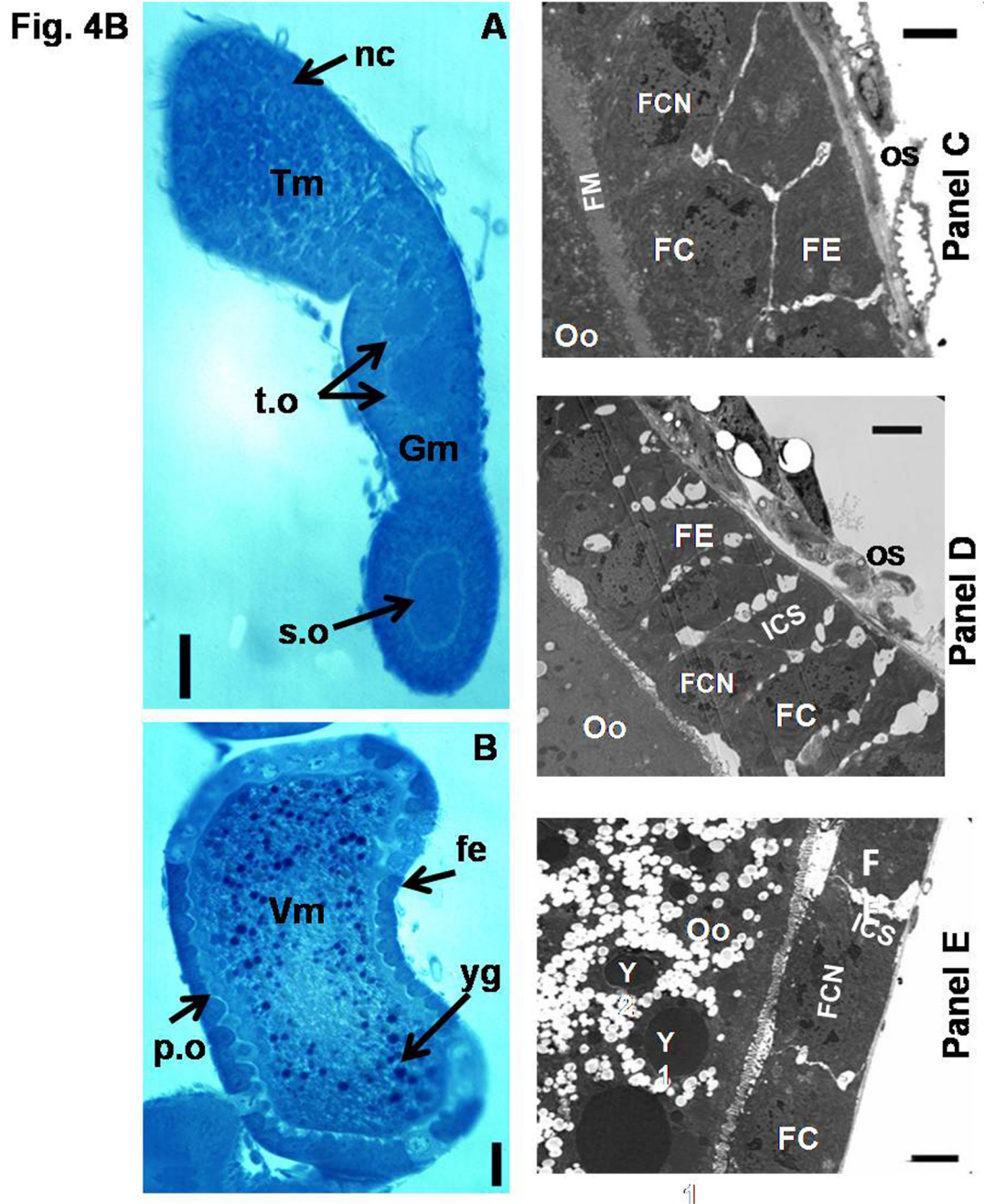
Fig. 4.

Fig. 4A. Progression of primary oocyte maturation during 60–102 h PAE. The ovaries were dissected at specific time-points and stained with nuclear stain, DAPI. The representative ovariole(s) at specific time-points are shown (panels a–f). The staging of the primary oocyte (yellow arrow) in the each ovariole was based on Ullmann (1973). The focus is on the staging of the primary oocyte. For distinct regions of the ovaries, see Fig. 4B. Note the increase in size of the primary oocyte at Stage 3 at 72 h PAE (panel b). The oocyte is spherical with follicular epithelial layer at Stage 4 at 84 h PAE (panel c). The oocyte becomes elongated surrounded by a monolayer of follicular cells at Stage 5 (panels d &e).

Many follicular epithelial cells surrounding the mature oocyte are observed at Stage 6 (panel f). Scale Bar: 100 µm.

Fig. 4B. Light and Electron micrographs depicting the mature ovariole and the changes in the follicular epithelium of the primary oocytes (A–E). Light micrographs of oocytes/ovarioles stained with Methylene Blue. Semithin longitudinal sections of ovariole on day 5 PAE (A & B). Fe, follicular epithelium; nc, nurse cells; p.o, primary oocyte; s.o, secondary oocyte; t.o, tertiary oocyte; yg, yolk granules; Tm, tropharium; Gm, germarium; Vm, vitellarium.N=4 Scale Bar: A & B − 50 µm. Electron micrographs of a portion of the primary oocyte (C–E). Follicle epithelial cells organize into a columnar epithelium at Stage 5 (C). Note the intercellular spaces appearing between the follicle cells at Stage 6 (D). Yolk deposition was observed in the oocyte and the follicle cells flatten at Stage 7 (E). FC, Follicle cells; FE, Follicular epithelium; FCN, follicle cell nucleus; FM, Follicle membrane; ICS, Intercellular spaces; Oo, Primary oocyte; Os, ovarian sheath; Y, Yolk granules. Scale Bar: 2 µm.

Fig. 5A
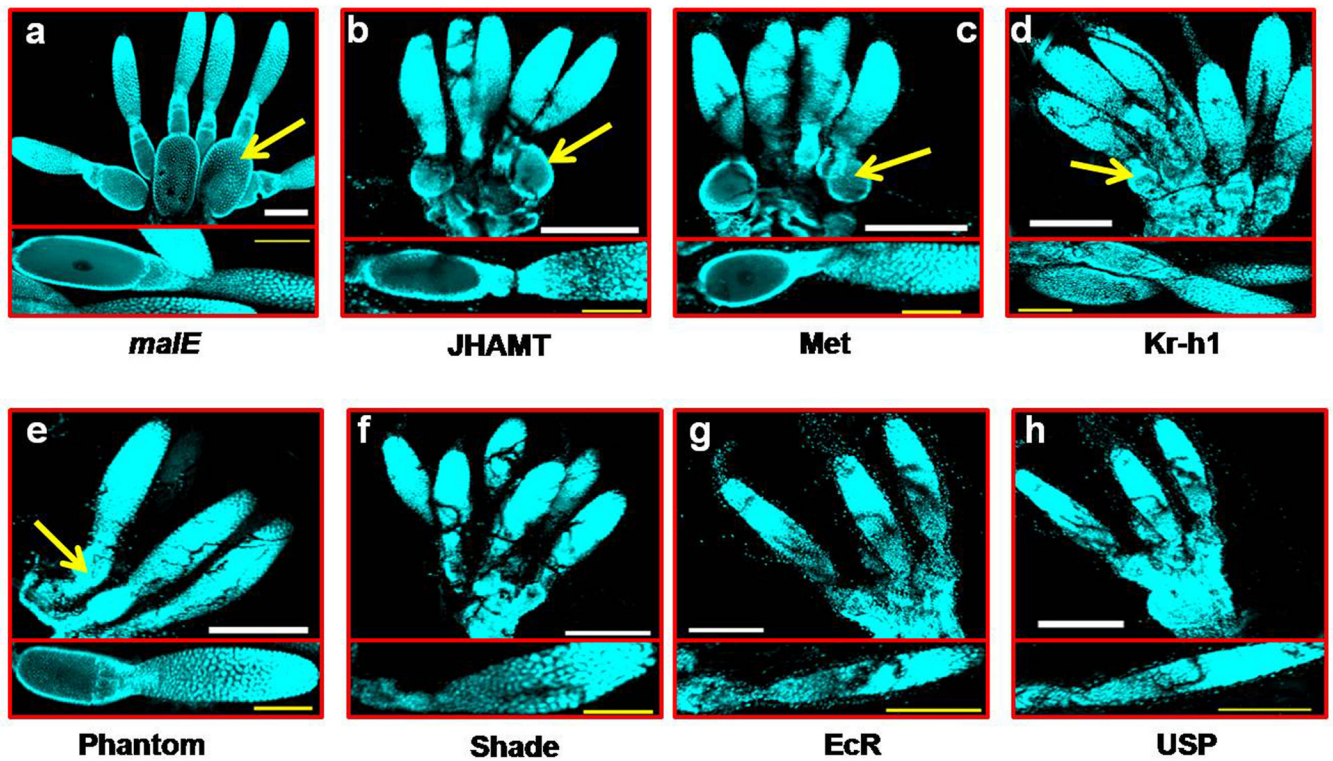
Fig. 5B
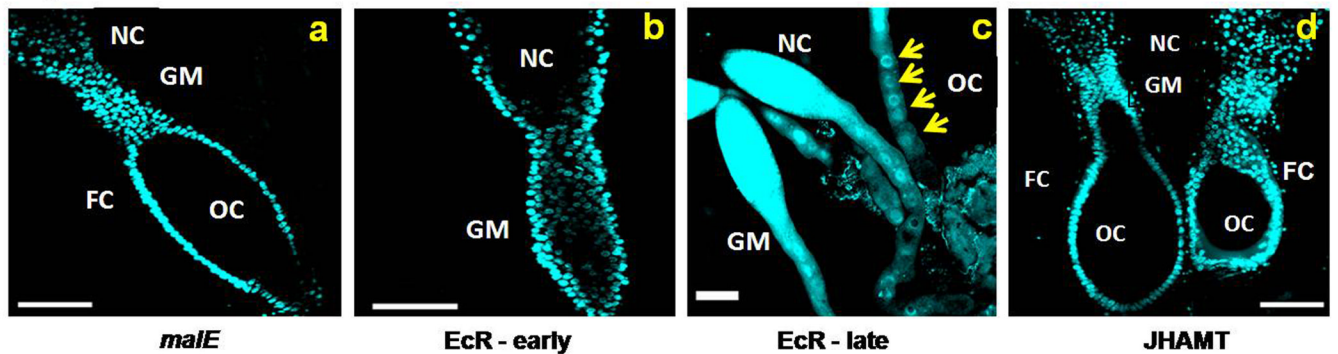
Fig. 5.

Fig. 5A. Ovarian growth and primary oocyte maturation in the RNAi insects (panels a–h). JHAMT, Met, Kr-h1, and *malE* (control) dsRNA were injected into two-day-old female pupa. Phantom, Shade, EcR, USP, and *malE* (control) dsRNA were injected into female beetles on day 0 PAE soon after emergence (within 24 h of emergence). The ovaries were dissected on day 4 PAE in both cases and stained with DAPI. A representative ovary/ ovariole was shown from the control insects (panel a). Each panel represents one of the pair of ovaries of experimental insects and the insert at the bottom shows a single ovariole of the ovary to highlight the stage of the primary oocyte. The ovary in each panel is aligned with nurse cells on top and oocyte at the bottom. The ovariole in each insert are aligned with

nurse cells to the right and the primary oocyte to the left. The mature primary oocytes are marked with yellow arrow. N=10. Scale Bar: 200 µm (white); 100 µm (yellow).

Fig. 5B. A portion of ovariole of *malE* (control), EcR, and JHAMT RNAi insects. dsRNA of the above genes were injected as mentioned in legend for Figure 5A. The ovaries were dissected on day 4 PAE and stained with DAPI (panels a–d). The ovariole of control insects (panel a) showed well developed primary oocyte (OC) surrounded by a monolayer of follicle cells (FC). The germaruim (GM) and nurse cells (NC) are seen above. EcR RNAi beetle ovariole on day 4 PAE (panel b) showed the absence of mature primary oocyte, while on day 8 PAE (panel c) showed several small oocytes. JHAMT RNAi ovariole (panel d) was similar to the control insect ovariole. N=10. Scale Bar: 100 µm.
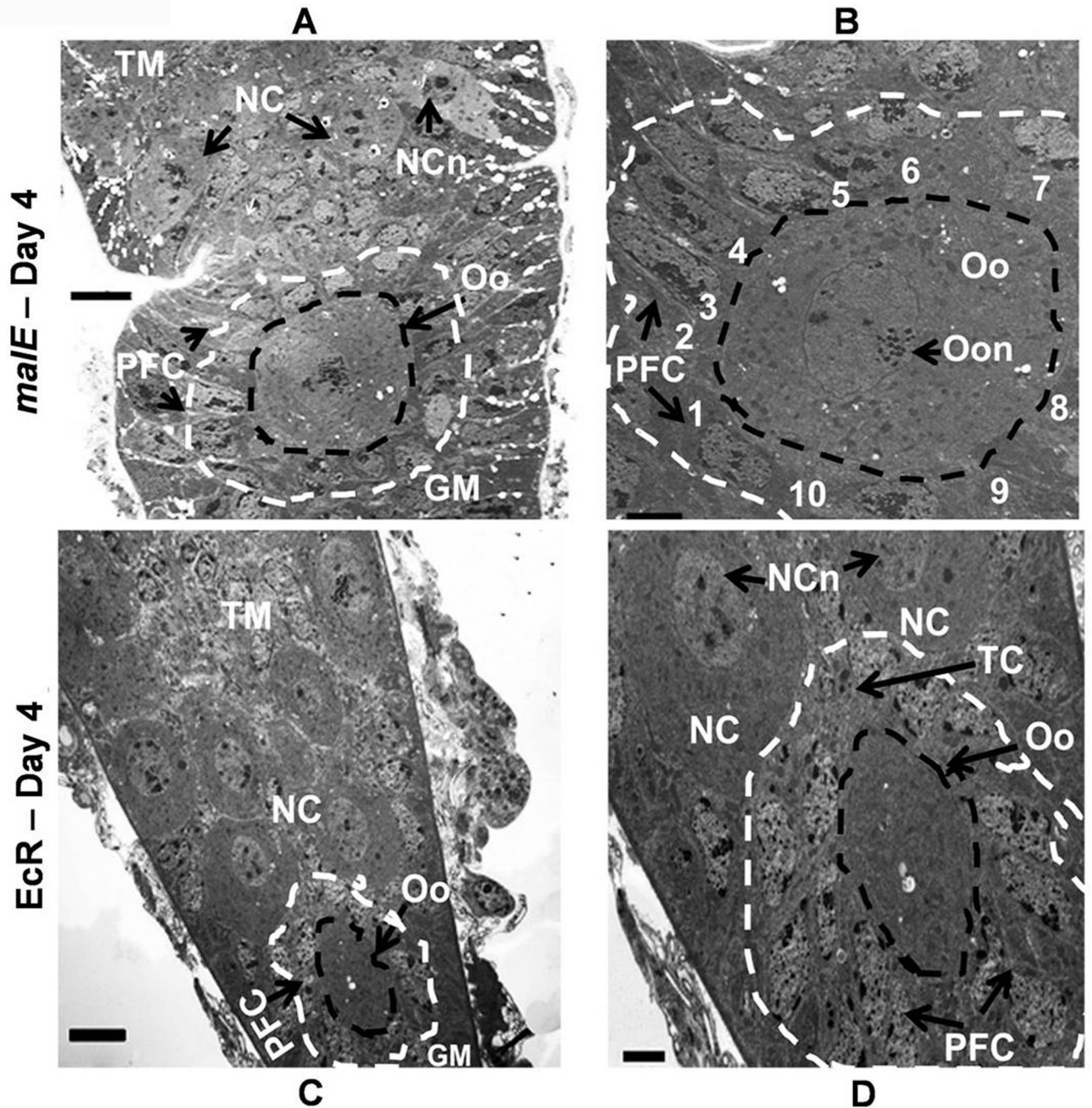
Fig. 6.
Ultrathin longitudinal section of the ovariole showing oocyte development at different stages in the germarium of *malE* RNAi (control, A & B) and EcR RNAi (C & D) on day 4 PAE. Panel A, Neck region showing germarium with developing secondary oocyte surrounded by follicular cells; Tropharium with nurse cells occupy the distal portion of the germarium; black circle- boundary of the secondary oocyte; White circle- boundary of the surrounding follicle cells. Panel B, Enlarged circled area of A with the follicle cells surrounding the secondary oocyte is numbered 1–10. Panel C, Germarium and tropharium regions of EcR RNAi beetle ovariole; Black circle, boundary of the primary oocyte; White circle- boundary of the surrounding follicle cells. Panel D, Germarium region circled in C at higher

magnification; the primary oocyte is surrounded by follicular cells; also seen are trophic cards and nurse cells. GM, Germarium; NC, Nurse cells; NCn, Nurse cell nucleus; Oo, Oocyte; Oon, Oocyte nucleus; PFC, follicular cell; TC, Trophic card; TM, Tropharium. All micrographs are arranged with tropharium on the top and germarium towards the bottom. N=4. Scale Bar: A,C − 5 µm; B, D − 2 µm.

Table 1

Gene expression in the ovary Vs whole body of female beetles on day 4 PAE by microarray analysis

Gene ID	Ovary 4 day PAE	Whole body 4 day PAE	Fold change	p-value	Annotation
Vitelligenin receptors					
TC004042	5.525579	0.846001	6.53141	0.000237	VgR1
TC008425	4.12203	1.03703	3.97483	0.000683	VgR2
20E biosynthesis and action					
TC011231	4.054114	1.131469	3.583052	1.77E-05	Shade
TC014274	3.762641	1.076641	3.494796	3.86E-05	Shadow
TC001916	3.180004	0.991075	3.208642	0.000386	Phantom
TC015030	3.52548	1.102684	3.197181	1.82E-05	Spookier-related
TC004159	4.223212	1.368588	3.085817	0.00384	Spookier
TC014691	2.358138	0.874333	2.697071	0.000155	Disembodied
TC012113	2.530572	0.964173	2.624605	0.000295	EcR
TC003935	2.28661	1.131274	2.02127	0.00278	E78
TC004598	2.576739	0.920134	2.800394	0.000224	HR78
JH metabolism					
TC003437	5.70203	0.70476	8.090737	0.00302	JHEH
TC002992	2.627899	0.833283	3.153668	0.000894	JHEH
TC013193	2.09687	0.75478	2.778123	3.82E-05	JHE

The total RNA isolated from the whole body and ovary of the female beetle at 4 day post adult emergence (PAE) were used for microarray analysis. The data filtered using Benjamini-Hochberg false discovery rate multiple testing corrections generated by GeneSpring GX v.9.0.1 software were used. The normalized expression levels of selective genes involved in vitellogenesis, JH and 20E pathways at different fold changes (whole body Vs ovary) with p-value of less than 0.05 for each gene are shown for comparison.

Table 2

Putative ovarian specific genes identified by microarray analysis

Gene ID	Whole body	Ovary	p-value	Fold change	Annotations	Drosophila homologues	Homology	GO predictions *
TC000385	0.900734	1.675632	0.00011	1.86	hemipterous	FBgn0010303	1e-74	ovarian follicle cell development
TC016112	0.829332	1.607096	4.17E-05	1.94	mago nashi	FBgn0002736	3e-70	ovarian differentiation, ovarian axis determination, ovary development, ovary construction
TC009471	1.07281	1.686216	0.00945	1.57	unknown	FBgn0041252	3e-146	ovarian follicle cell development
TC011262	1.075502	4.431458	5.90E-05	4.12	RNA-binding protein	FBgn0004882	1e-109	ovarian differentiation, ovarian axis determination, ovary development, ovary construction
TC007589	1.010175	1.794957	0.00517	1.78	unknown	FBgn0000352	8e-109	cell differentiation
TC08711	1.107473	2.409955	0.000167	2.18	piwi	FBgn0000416	2e-103	ovarian follicle cell development
TC004803	1.274082	1.847736	0.00189	1.45	unknown	FBgn0010269	1e-91	ovarian follicle cell development
TC003416	1.087195	3.378076	8.59E-05	3.11	unknown	FBgn0000996	2e-75	ovarian follicle cell development
TC011220	0.932557	3.290737	2.94E-05	3.53	unknown	FBgn0004399	0.0	ovarian differentiation, ovarian axis determination, ovary development, ovary construction
TC011200	1.090485	2.798275	0.000196	2.57	unknown	FBgn0025815	0.0	ovarian follicle cell development
TC010546	0.866453	2.179812	0.000112	2.52	unknown	FBgn0041164	4e-161	ovarian follicle cell development, ovarian differentiation, ovarian axis determination, ovary development, ovary construction
TC014516	1.125096	1.867786	0.000177	1.66	spindle E	FBgn0003483	2e-52	oocyte maturation, ovarian follicle cell development
TC010103	1.235231	3.683558	9.01E-05	2.98	vasa	FBgn0003970	4e-133	Oocyte fate determination, germarium derived oocyte differentiation
TC014860	0.699707	1.130912	0.000433	1.62	unknown	FBgn0086384	4e-105	ovarian differentiation, ovarian axis determination, ovary development, ovary construction

The total RNA isolated from the whole body and ovary of the female beetle at 4 day post adult emergence (PAE) were used for microarray analysis. The data filtered using Benjamini-Hochberg false discovery rate multiple testing corrections generated by GeneSpring GX v.9.0.1 software were used. The normalized expression levels of selective genes involved in at different fold changes (whole body Vs ovary) with p-value of less than 0.01 for each gene are shown.

*
Gene Ontology (GO) predictions in *D. melanogaster* were based on Baker and Russell (2009).